

# CELLULAR AUTOMATON FOR THE FRACTURE OF ELASTIC MEDIA

PETER OSSADNIK

*HLRZ, KFA Jülich*

*Postfach 1913, D-5170 Jülich, Germany*

We study numerically the growth of a crack in an elastic medium under the influence of a travelling shockwave. We describe the implementation of a fast algorithm which is perfectly suited for a data parallel computer. Using large scale simulations on the Connection Machine we generate cracks with more than 10000 sites on a  $1024 \times 1024$  lattice. We show that the resulting patterns are fractal with a fractal dimension that depends on the chosen breaking criterion and varies between 1. and 2.

## 1. Introduction

How does a solid body break under an externally applied load? This is an important question for researchers in many fields and has strong implications on e.g. materials science, engineering or geophysics. It has been studied for a long time quite extensively using numerical, experimental and analytical methods.<sup>1</sup>

If one considers the solid to be a linear elastic medium the formulation of the initial question can be made in terms of the Lamé equation

$$(1 - 2\nu)\Delta\underline{u} + \nabla(\nabla \cdot \underline{u}) = 0 \quad (1)$$

which describes the displacement  $\underline{u}$  of a small volume element in an elastic material from its equilibrium position. The Poisson ratio  $\nu$  is a material dependent parameter which has the following meaning: If one applies a uniaxial force to an elastic bar of length  $L$  and cross section  $W \times W$ , it will not only change its length by  $\Delta L$  in the direction of the force, but it will also change its width by  $\Delta W$  in the direction perpendicular to the force. The Poisson ratio then defines the relative amount of change

$$\nu = -\frac{\Delta W/W}{\Delta L/L}. \quad (2)$$

Due to thermodynamical reasons  $\nu$  is bounded between  $-1 \leq \nu < 0.5$ . Concrete for instance has a Poisson ratio  $\nu \approx 0.2$ .

A crack in such a system can be described as an additional force free surface which thus obeys the boundary condition

$$\underline{\underline{\sigma}} \cdot \underline{n} = 0 \quad (3)$$

where  $\underline{\underline{\sigma}}$  is the stress tensor and  $\underline{n}$  is a surface vector. The crack grows if the stress parallel to the crack surface  $\sigma_{\parallel}$  is larger than a certain material dependent critical stress  $\sigma_C$ . Since no first principle law for the normal growth velocity is known one assumes the general behavior

$$v_n \propto (\sigma_{\parallel} - \sigma_C)^\eta \quad (4)$$

where  $\eta$  is often simply set to unity. The equations (1), (3) and (4) formulate the growth of a crack as a moving boundary problem which is far more difficult to solve than the Lamé equation itself. Yet, there is one important property of real material missing, which is “disorder”. Microscopically disorder means deviations from the perfect crystal structure of the elastic material due to vacancies, dislocations or grain boundaries. But macroscopically these imperfections are simply reduced to spatial randomness of the material properties like Poisson ratio and breaking threshold.

In numerical simulations for crack growth one often discretizes the elastic medium on a lattice, for instance with a finite element scheme.<sup>2</sup> According to the chosen boundary conditions and the externally applied load one relaxes the system to equilibrium. Then one picks one or several bonds according to a given rule – for instance the bond with the highest load – and breaks it. This defines a new boundary and therefore one has to resolve the whole problem again. This procedure is then repeated until a crack of desired size is grown. The disorder is often put into the simulations by considering lattice parameters (like bond strength and breaking threshold) that vary from site to site. Since the system has enough time to relax to full equilibrium before the crack can grow, such a procedure is only capable of describing quasi static processes.

On the other hand there are phenomena — like explosions, shattering of glass or shock waves – which should not be treated in a static approximation and in which the system is not able to relax to equilibrium before breaking a bond, but in which the time to relax the system is comparable to or larger than the time one needs to propagate the crack. Such a situation usually results in cracks with many sidebranches growing behind the shock front since the internal energy cannot be dissipated fast enough.<sup>3</sup> In the following we are going to study numerically such a process in which one obviously has to take into account the dynamical behavior of the elastic medium.

The organization of this paper is thus as follows: in Sect. 2 we introduce the general model, whose implementation on the Connection Machine is described in Sect. 3. In Sect. 4 we describe the details of the simulation and in Sect. 5 we present some results.

## 2. The Model

As a model for the elastic material we consider a triangular network of Hookean

springs connecting points of mass  $m$ . A triangular network is necessary for the simulation since a simple quadratic lattice does not have any shear modulus and thus can be deformed arbitrarily under shear load. This model is known as “central force model”<sup>2</sup> since the Hookean springs are isotropic. The boundary sites of this network are kept fixed in space. On each site there are two continuous degrees of freedom, which are the coordinates of the displacement  $u_x$  and  $u_y$  of this site from its equilibrium position  $\underline{r}_0$ . Since we want to study the dynamical behavior of this network we have to determine the time evolution of the displacements which is governed on each lattice site by Newton’s equation. Following a suggestion of Chopard<sup>4</sup> we use a discrete time Hamilton formalism to express the dynamic behavior. The Hamiltonian of this system is given by

$$H(\underline{p}_1 \cdots \underline{p}_N, \underline{r}_1 \cdots \underline{r}_N) = \sum_{i=1}^N \frac{p_i^2}{2m_i} + \frac{1}{2} \sum_{i,j=1}^N U_{ij}(\underline{r}_i, \underline{r}_j) \quad (5)$$

where  $\underline{p}_i$  and  $\underline{r}_i$  are the momentum and position of site  $i$ , and  $U_{ij}$  is the interaction energie between two lattice sites  $i$  and  $j$ .  $U_{ij}$  is nonzero only between nearest neighbor sites and since we use Hookean springs it is simply a harmonic potential

$$\begin{aligned} U_{ij} &= \frac{k_{ij}}{2} (|\underline{r}_i - \underline{r}_j| - a)^2 = \frac{k_{ij}}{2} (|\underline{u}_i + \underline{r}_{0i} - \underline{u}_j - \underline{r}_{0j}| - a)^2 \\ &= \frac{k_{ij}}{2} (|\underline{u}_i - \underline{u}_j + \underline{dr}_{ij}| - a)^2 \end{aligned} \quad (6)$$

where  $k_{ij}$  is the coupling constant between the sites  $i$  and  $j$ .  $\underline{dr}_{ij} = \underline{r}_{0i} - \underline{r}_{0j}$  is the vector between their equilibrium positions and  $a$  is the equilibrium length of the connecting spring (please note, that  $\underline{dr}_{ij}$  does not mean differentials). In our simulation we are going to set  $a = 0$  while we keep  $\underline{dr}_{ij} = 1$ . This corresponds to the case of a prestretched network and can be compared for instance with the skin of a drum. The discretized versions of Hamilton’s equations are

$$\begin{aligned} \underline{r}_i(t+1) - \underline{r}_i(t) &= \frac{\partial H}{\partial \underline{p}_i} = \frac{\underline{p}_i(t)}{m_i} \\ \underline{p}_i(t) - \underline{p}_i(t-1) &= -\frac{\partial H}{\partial \underline{r}_i} \end{aligned} \quad (7)$$

where we use vector derivatives as symbols for the corresponding gradients. The time evolution of the displacement field can finally be written as

$$\begin{aligned} \underline{u}_i(t+1) - 2\underline{u}_i(t) + \underline{u}_i(t-1) &= -\frac{1}{m_i} \frac{\partial H}{\partial \underline{u}_i(t)} \\ &= \sum_{j=NN(i)} k_{ij} \cdot \underline{\delta}_{ij} \cdot \left(1 - \frac{a}{|\underline{\delta}_{ij}|}\right) \end{aligned} \quad (8)$$

where  $\underline{\delta}_{ij} = \underline{u}_i(t) - \underline{u}_j(t) + \underline{dr}_{ij}$ . This equation (8) defines the updating rule, which relates the displacements at time  $t+1$  to the displacements at times  $t$  and  $t-1$ .

Although the chosen dynamics seems to be rather crude as compared to molecular dynamics, one can actually show that it conserves the total momentum and some kind of total “energy”. Moreover we show that it conserves the essential features we need for the generation of cracks: A wave packet that is imposed on the lattice will travel with only minor changes in shape with a definite velocity through the lattice.

### 3. The Growth Model using Fortran 90

Since the same updating rule (8) is applied to all lattice sites at each time step and on the other hand the topology of the underlying lattice is, in contrast to molecular dynamics, not changed due to rearrangements of particles single instruction multiple data (SIMD) machine like the CM is the appropriate computer architecture for this problem: Each lattice site is mapped onto one virtual processor and all sites are updated in parallel. The only inter processor communication is required for the calculation of the right hand side of eqn. (8). But because the triangular lattice structure can be mapped onto a square lattice with next nearest neighbor interactions into one direction, a nearest neighbor grid communication using `CSHIFTS` is sufficient and no general router communication is required, which makes this lattice model fast and efficient.

In the actual implementation of the program we chose the following data layout for the main variables: Each processor has to store the displacements at time  $t$  and  $t - 1$ , `UT` and `UTM1`, which are represented as complex numbers. Since we intend to simulate a “disordered” system, we assign to each spring a different, randomly chosen coupling constant. Therefore we keep on each lattice site the six couplings `K` to all neighbors. By doing this we waste some memory space because each  $k_{ij}$  is stored twice – on site  $i$  and on site  $j$  – but we save computer time by avoiding unnecessary communication. The data layout for the main variables is thus as follows

```

      COMPLEX , ARRAY (NXY, NXY)   :: UT, UTM1
      REAL    , ARRAY (Z, NXY, NXY) :: K
      CMF$ LAYOUT UT(:NEWS, :NEWS)
      CMF$ LAYOUT UTM1(:NEWS, :NEWS)
      CMF$ LAYOUT K(:SERIAL, :NEWS, :NEWS)

```

Listing 1.

The `LAYOUT` directive for `K` is used to group the couplings of one site as a serial dimension onto one processor. It is necessary, because otherwise the compiler would spread the couplings over all virtual processors which results in unnecessary communication for the force calculation. Using this data layout a single step of the updating rule (8) is programmed in a straightforward manner in CM Fortran

```

      C      GET VECTORS TO NEIGHBORS
      C      COMPUTE NEW PARTICLE POSITION AND MOMENTUM
      C      NN is a help field to store r_i-r_j. It has the same layout as

```

```

C      ut and utm1.
      NN(1, :, :) = CSHIFT(UT,1,1)
      NN(2, :, :) = CSHIFT(UT,2,1)
      NN(4, :, :) = CSHIFT(UT,1,-1)           !get displacements
      NN(5, :, :) = CSHIFT(UT,2,-1)           !of nearest neighbors
      NN(3, :, :) = CSHIFT(NN(4, :, :),2,1)
      NN(6, :, :) = CSHIFT(NN(1, :, :),2,-1)
      NN(1, :, :) = NN(1, :, :)-UT+DR_1
      NN(2, :, :) = NN(2, :, :)-UT+DR_2
      NN(3, :, :) = NN(3, :, :)-UT+DR_3
      NN(4, :, :) = NN(4, :, :)-UT+DR_4           !calculate difference vector
      NN(5, :, :) = NN(5, :, :)-UT+DR_5
      NN(6, :, :) = NN(6, :, :)-UT+DR_6
      UTM1 = SUM(NN*(K*(1.-A1/ABS(NN))),DIM=1)/M + 2.*UT - UTM1

```

Listing 2.

The CSHIFT commands are used to communicate the displacements between “neighboring” processors. By carefully reusing already shifted data it is of course possible to get the displacements from the six nearest neighbors on the triangular lattice with only six CSHIFTS. Since we are not using full next nearest neighbor communication the use of stencil operations does not seem useful at this point. The global SUM along the first dimension computes the total force exerted onto each site by its neighbors. Because the first dimensions of the coupling constant array  $\mathbf{k}$  and the vectors to the nearest neighbors NN are laid out onto the same processor as a `:serial` dimension, the computation of the SUM does not require any communication.

Unfortunately this simple formulation does not give optimal performance. The compiler allocates and deallocates unnecessary temporary fields and even generates general `CM_send` router communication, which in fact uses 43% of the total CPU time! To obtain a much better performance we coded the code fragment shown in Listing 2 completely in PARIS (PARallel Instruction Set). This allows to fully control the memory allocation, the communication and to make efficient use of pipelined commands like `CM_f_sub_const_mult_always`. Now, most of the CPU time – 38% – is used for the calculation of the distance between neighboring lattice sites  $|\underline{r}_i - \underline{r}_j|$  which is coded as `CM_f_c_abs_2`. Now, the NEWS communication part is negligible and sums up to 5.8% of the total CPU time.

These improvements result in a speedup of a big factor of five as compared to the straightforward implementation. One obtains on 8K processors of the previously described CM2 an update rate of 1.1 millions of updates per second (MUPS) and a speed of 110 MFlops. As a comparison, one can obtain with typical spin cellular automata using multispin coding techniques more than 1000 MUPS on one processor of a NEC-SX3<sup>5</sup> and on a CM2-16K a Q2R cellular automaton runs at 1600 MUPS.<sup>6</sup> For a full molecular dynamics simulations on an CM200-8K Hedman and Laaksonen achieve about 0.2 MUPS<sup>7</sup> and for MD simulations on a CM2-16K Mel'čuk et. al.

obtained an update rate of 4.5 KUPS.<sup>8</sup>

#### 4. The simulation

All simulations are performed on a  $1024 \times 1024$  lattice and we use between 3000 and 5000 timesteps. At the beginning of the simulation the couplings are chosen at random out of a uniform distribution with mean value  $k_0 = 0.005$  and a width of typically 50%. To initiate the crack growth we break all bonds between site  $\underline{r}_0$  and its neighbors. Afterwards an initial pulse is imposed on the center of the lattice: If  $\underline{r}_0$  is the central site in the lattice, then its nearest neighbors  $\underline{r}_1 \dots \underline{r}_6$  are displaced radially outward for 100 lattice units while keeping all other sites fixed. This displacement seems very large at first sight, but since we use a harmonic potential between the sites the actual size of the initial displacement is not relevant. We only wanted to make sure that this perturbation is much larger than the “thermal” motion unduced by chosing random coupling constants. At time  $t = 0$  all sites are released and the system is free to evolve. After every other time step one looks for the bond with the largest elongation  $l_m$ . Then one determines all bonds whose elongations  $l$  are larger than  $\alpha \cdot l_m$  – where  $\alpha$  is an adjustable parameter – and which lie on the surface of the already existing crack. All those bonds are broken by setting the corresponding coupling constant  $k_{ij}$  to zero. Here one has to notice that this breaking rule does not require any communication and can be performed completely in parallel since both sites  $i$  and  $j$  which are connected by such a bond will clear their own copy of  $k_{ij}$ .

Thus we consider a relative breaking threshold rather than an absolute one, which has the following reason: In an absolute breaking threshold one would break all bonds whose elongation is larger than some fixed critical length  $l_c$ . On the other hand the amplitude of the outgoing wave packet is decreasing with the distance from the center. So, when the wave packet has initially an amplitude that is larger than the threshold, the outgoing wave will break all bonds it reaches until its amplitude has dropped below the threshold and from then on no further bond will be broken. Thus, one only creates a structureless isotropic hole in the center of the system.

A somewhat similar model has been studied by Louis et. al.<sup>9</sup> They try to solve a quasi static problem, but perform only a few relaxation steps to find the equilibrium state of the network. However, since they use an overrelaxation scheme the relaxation of their system towards equilibrium has another dynamical interpretaion than the iterative method I use. Another similarity is given in the breaking rules. Louis et. al. pick bonds that are to be broken with a probability that is proportional to the bond length  $P_{ij} \propto |\underline{r}_i - \underline{r}_j|$ .

#### 5. Results

To demonstrate that the dynamics (8) produces reasonable results we first consider the case of a smooth wave packet travelling through a system without disorder and without breaking. Therefore we applied not a singular pulse to the network but

rather a smooth wave packet. The initial radial displacements of the central sites are

$$\underline{u}(t) = \underline{u}_0 \cdot \left(1 - \cos\left(2\pi \cdot \frac{t}{\tau}\right)\right) \quad (9)$$

for  $0 \leq t \leq \tau$  and  $\underline{u}(t) = 0$  for  $t > \tau$  while all other sites are free to move. The period is chosen to be  $\tau = 100$ .

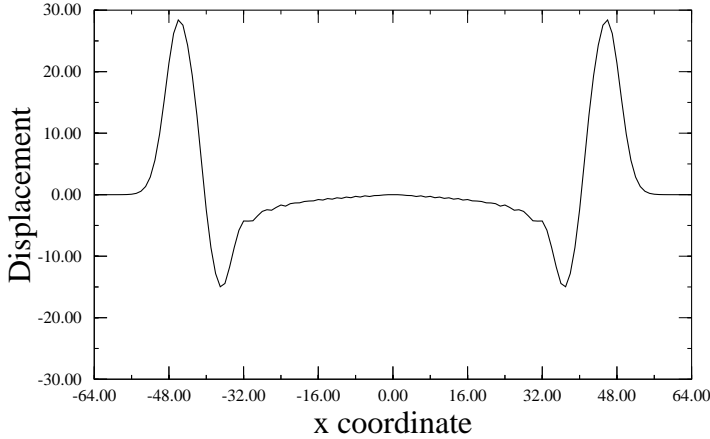


Fig. 1. Cut through a shockwave after 200 timesteps.

Fig. (1) shows a cut along the x axis through this wave packet at time  $t = 200$ . One indeed recovers the original pulse plus a further minimum which is due to the fact that we keep the displacements of the central sites for  $t > \tau$  fixed at zero. Because of their inertia the neighboring sites keep vibrating which results in the second minimum. If one measures the velocity of the maximum of the wave packet one obtains a value which agrees with the analytical expression for the group velocity of a circular wave with frequency  $\omega = 2\pi/\tau$  on a triangular lattice.

After having confirmed that the travelling wave shows reasonable behavior we restrict ourselves again to the case of a singular pulse, which corresponds to the case  $\tau = 2$ .

Fig. 2. Crack patterns generated for (from left to right) a)  $\alpha = 1$ , b)  $\alpha = 0.98$  and c)  $\alpha = 0.95$ .

In figs (2.a-2.c) we show examples of cracks which were generated for different breaking thresholds:  $\alpha = 1$  (10934 sites) – which means that only the bond with the largest elongation is broken –  $\alpha = 0.98$  (16038 sites) and  $\alpha = 0.95$  (35837 sites). The number in brackets are the number of sites that are “connected” by broken bonds. All cracks show a starlike and fractal structure. For decreasing  $\alpha$  they become more and more ramified. This is easily understood since with decreasing

$\alpha$  many more bonds are eligible to be broken. The delta-like excitation we impose initially on the lattice is highly non-periodic and therefore produces waves with many different frequencies, although lower amplitude. For small enough  $\alpha$  many of these waves can contribute to the growth of the crack. But one also has to take into account another effect. Since the lattice is prestretched each bond that is broken is a source for another spherical wave travelling away from this point. For small enough  $\alpha$  also those waves can break bonds and therefore can lead to an avalanche-type growth of the crack. Thus, one can distinguish two different regimes: For  $\alpha$  close to unity the crack grows mainly at the tips at the outer branches which coincide with the front of the shockwave. The sidebranches behind the shockfront remain inactive. For smaller  $\alpha$  also the tips behind the shockfront continue to grow and split and eventually the crack becomes space filling.

Another fact to be noticed is that for decreasing  $\alpha$  the lattice structure becomes more and more dominant and eventually the cracks grow into a structure with sixfold symmetry.

To be more quantitative, we study the dependence of the number of broken bonds  $N$  on the radius of the cluster, which is measured in terms of the radius of gyration  $R_G$ .  $R_G$  describes the average distance of all broken bonds from the center of mass  $\mathcal{L}_{CM}$  of the crack

$$R_G = \sqrt{\sum_{i=1}^N (r_i - \mathcal{L}_{CM})^2}. \quad (10)$$

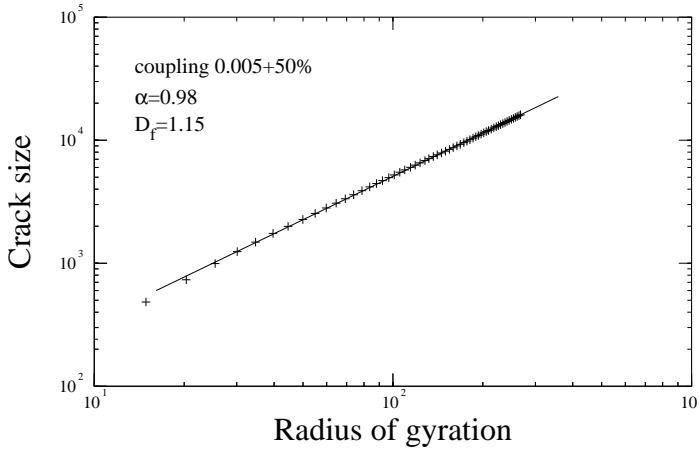


Fig. 3. Scaling of the number of broken bonds with the radius of the crack.

In fig. (3) we show the typical behavior of the number of broken bonds. As an example we show data for  $\alpha = 0.98$  in which we averaged over four cracks.



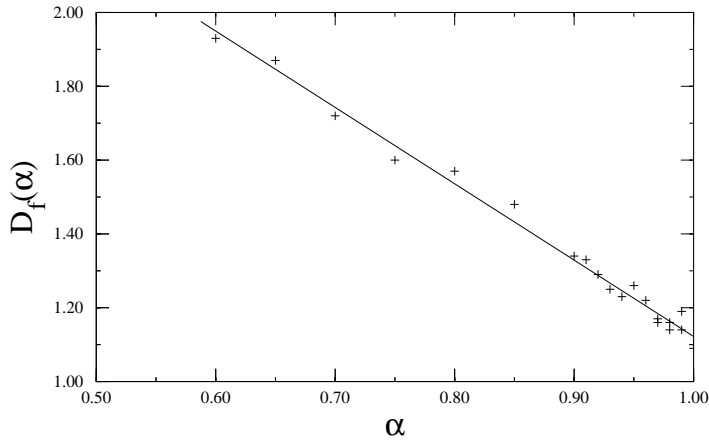


Fig. 4. Dependence of fractal dimension on the breaking threshold.

One finds that this number has a power law dependence on the radius of gyration

$$N \propto R_G^{D_f} \quad (11)$$

and for this specific example we find a fractal dimension  $D_f = 1.15$ . As indicated above this exponent varies with varying  $\alpha$ . So, in fig. (4) we show all exponents  $D_f$  for different  $\alpha$ .

Also in this plot the exponents  $D_f(\alpha)$  were obtained by averaging over four independent realizations. One obtains a linear dependence

$$D_f(\alpha) = -(2.06 \pm 0.05) \cdot \alpha + (3.19 \pm 0.05). \quad (12)$$

Thus, for decreasing  $\alpha$  one approaches a space filling structure which one reaches for  $\alpha \approx 0.58$ . However, it could be possible that for even larger clusters the asymptotic behavior changes and one crosses over into other exponents  $D_f$ .

## 6. Conclusions

We have described the implementation and results of a discrete time simulation for the growth of large cracks on a triangular network. We use a central force model and study the dynamical behavior of crack growth instead of studying the slow growth modes. Using a simplified dynamics, which anyway reproduces the essential features for the crack production, we are able to grow cracks with more than 10000 sites on a  $1024 \times 1024$  lattice. We obtain fractal growth patterns with dimensions almost in the whole range between 1.1 and 2.0. The dimensionality of the cracks is mainly governed by the breaking threshold  $\alpha$  and one finds a linear dependence of

$D_f$  on  $\alpha$ .

## References

1. For recent reviews see *Statistical Models for the Fracture of Disordered Media*, eds. H. J. Herrmann, and S. Roux (North-Holland, Amsterdam, 1990); *Disorder and Fracture — Proc. NATO ASI*, eds. J. C. Charmet, S. Roux, and E. Guyon, (Plenum Press, New York, 1990); H. J. Herrmann, in *Fractals and Disordered Systems*, eds. A. Bunde, and S. Havlin, (Springer, 1990).
2. E. Schlangen, J. G. M. van Mier, in *Proc. Int. EPRI. Conf. on Dam Fracture*, eds. V. E. Saouma et. al., 1991; S. Feng, P. N. Sen, *Phys. Rev. Let.* **52**, 216(1984); S. Roux, E. Guyon, *J. Physique. Let.* **46**, L999(1985)
3. E. H. Yoffe, *Phil. Mag.* **42**, 739(1951), Lord Rayleigh, *Proc. Lond. Math. Soc.* **17**, 4(1885)
4. B. Chopard, *J. Phys. A* **23**, 1671(1990); N. H. Margolus, Ph. D. Thesis, MIT, 1987.
5. R. W. Gerling, D. Stauffer, *Int. J. Mod. Phys. C* **2**, 799(1991)
6. S. C. Glotzer, D. Stauffer, S. Sastry, *Physica A* **164**, 1(1990)
7. F. Hedman, A. Laaksonen, in *Large Scale Computations in Quantum Chemistry and Physics — Proc. Namur SCF Conf.*, eds. J. M. André et. al., (special issue of Int. J. Quant. Chem., 1992), to appear
8. A. Mel'čuk, R. Giles, and H. Gould, *Computers in Physics* **May/June**, 311(1991).
9. E. Louis, and F. Guinea, *Europhys. Let.* **3**, 871(1987); P. Meakin, G. Li, L. M. Sander, E. Louis, and F. Guinea, *J. Phys. A* **22**, 1393(1989)